Published in final edited form as:
Metabolism. 2013 December ; 62(12): . doi:10.1016/j.metabol.2013.07.010.

Elevated adiponectin expression promotes adipose tissue vascularity under conditions of diet-induced obesity

Tamar R. Aprahamian
[1]Department of Medicine-Renal Section, Boston University School of Medicine, 650 Albany Street, X536, Boston, MA 02118, USA

Abstract

Objective—Despite the clinical prevalence of obesity, only recently has the importance of adipose tissue microenvironment been addressed at a molecular level. Here, I focused on the fat-derived cytokine adiponectin as a model system to understand the mechanism underlying adipose tissue vascularity, perfusion, inflammation, and systemic metabolic function.

Materials/Methods—Wild type, adiponectin-deficient, and adiponectin transgenic-overexpressing mice were maintained on chow diet or high fat/high sucrose diet for 32 weeks. Vascularization of adipose tissue was examined by confocal microscopy and perfusion was determined by recovery of injected microspheres. Adipose tissue inflammation and systemic metabolic function were also assessed.

Results—Modest over-expression of adiponectin led to a marked increase in adipose tissue vascularity and perfusion, and this was associated with diminished hypoxia and an increase in vascular endothelial growth factor-A (VEGF-A) expression in the obese mice. Adiponectin over-expression in diet-induced obese mice also led to the virtual absence of macrophage infiltration and the elimination of crown-like structures. Adiponectin transgenic mice also displayed a remarkable sensitivity to insulin and diminished hepatic steatosis. Under the conditions of these experiments, adiponectin deficiency did not diminish adipose tissue perfusion nor worsen metabolic function compared to wild type mice fed the high fat/high sucrose diet.

Conclusion—These data demonstrate that increased circulating adiponectin levels, and the obese environment, are associated with increased adipose tissue vascularization and perfusion, and improved metabolic function under conditions of long term diet-induced obesity.

Keywords

Angiogenesis; metabolic dysfunction; animal model

Send correspondence to: Tamar R. Aprahamian, Ph.D., Boston University School of Medicine, Department of Medicine-Renal Section, 650 Albany Street, 5th floor, Boston, MA 02118, Phone: +1 617 414 3368, Fax: +1 617 638 7326, aprahami@bu.edu.

Disclosure. The author declares no conflict of interest.

Author Contributions. TA was responsible for the design and conduct of the study, data collection and analysis, data interpretation, and manuscript writing.

Introduction

Recent studies have shown that total fat mass does not necessarily indicate metabolic status, leading to the concept that metabolic dysfunction is influenced not only by the quantity of adipose tissue but also by its quality [1]. Obesity leads to macrophage accumulation and high levels of the pro-inflammatory cytokine TNFα in the adipose tissue of humans and rodent models, which is correlated with the development of insulin resistance [2–5]. Correspondingly, inhibition of TNFα prevents insulin resistance [6–8]. The inflammatory status of adipose tissue is also affected by its perfusion by the microvessels [3, 4, 9]. Blood flow regulation is affected by increasing adipose tissue mass as well as enlargement of adipocytes [10]. Obese mice display capillary rarefaction in their fat pads and reductions in expression of the angiogenic growth factor VEGF, leading to adipose tissue hypoxia [11, 12]. In obese humans, adipose tissue inflammation and the imbalance of adipocyte-derived cytokines are correlated with increased cardiovascular risk and vascular injury [4, 9].

Adiponectin is an adipocyte-derived cytokine that is expressed at high levels by lean, healthy individuals, but its expression is diminished as body mass increases [13]. Large adipocytes, such as those found in obese subjects, produce less adiponectin and higher levels of pro-inflammatory cytokines including IL-6 and TNF-α [14]. In addition, these inflammatory cytokines and hypoxia can induce a reduction in adiponectin expression [3, 15, 16]. Cardioprotective effects of adiponectin include the ability to modulate vascular function and promote angiogenesis in ischemic skeletal muscle and tumors [17, 18]. Adiponectin also maintains an anti-inflammatory environment through its ability to inhibit T-cell proliferation, decrease co-stimulatory molecule expression of monocyte-derived dendritic cells, and facilitate macrophage clearance of apoptotic cells [19–22]. Transgenic mice over-expressing adiponectin have preserved insulin sensitivity and are protected from lipid accumulation after 48h of high calorie diet [23]. Furthermore, transgenic over-expression of adiponectin in the leptin-deficient *ob/ob* mouse protects against metabolic dysfunction, despite becoming severely obese [24]. Among the known functions of adiponectin, few, if any, studies have analyzed the role of adiponectin in the control of adipose tissue vascularity and microenvironment.

Here, adiponectin-deficient and –over-expressing mice were used as a model system to elucidate the associations among adipose tissue vascularity, inflammation, and systemic metabolic function. The purpose of this study was to determine the extent to which adiponectin impacts the adipose tissue microvasculature.

Methods

Mouse models and tissue collection—Adiponectin-deficient mice (apn-KO) on a C57 background were originally obtained from Dr. Yuji Matsuzawa [25]. Adiponectin transgenic over-expressing mice (apn-TG) were originally generated on an FVB background [26], were subsequently backcrossed to C57 [24], and obtained from Dr. Philipp Scherer. Wild type littermates served as controls. Mice were maintained on a chow diet or high fat/high sucrose diet (#F1850, BIO-SERV, 60% kcal from fat) starting at 8 weeks of age for 32 weeks. The epididymal fat pad (EFP) depot was collected, weighed, and subsequently divided in order to provide uniform tissue samples for further analyses. All experiments were approved by the Institutional Animal Care and Use Committee at Boston University.

Systemic metabolic properties—For insulin tolerance testing, an i.p. injection of human insulin (1.5U/kg body weight, Humulin R, Eli Lily) was administered to mice after an overnight fast. Blood glucose levels were measured using an Accu-Chek glucose monitor (Roche Diagnostics Corp.) and determined immediately before, and at intervals up to 120min after injection. Serum levels of free fatty acids were measured by a NEFA-HR(2)

microtiter procedure (Wako Diagnostics). Commercially available enzyme-linked immunosorbent assay kits were used to determine serum insulin (Crystal Chem Inc.), serum leptin (Crystal Chem Inc.), and serum adiponectin levels (B-Bridge International) according to the manufacturer's instructions.

Confocal Microscopy—To visualize the vasculature, 100ul of the isolectin Griffonia simplicifolia (Vector Labs) was administered to the circulation via cardiac injection 0.5hr before sacrifice. To visualize adipocytes, live, non-fixed EFP specimens were minced and incubated with BODIPY-Texas Red (Invitrogen) for 1hr followed by a brief PBS wash. Confocal microscopy was used to determine capillary density on tissue stacks with a 50μm thickness. Luminosity of isolectin (FITC)-labeled blood vessels was quantified for each mouse. Ten fields at 10x magnification were chosen at random for analysis.

Histology—A portion of the EFP was fixed in 10% formalin, embedded in paraffin, and sectioned. VectaStain kit (Vector Labs), anti-mouse Mac-2 (Cedarlane Labs) or perilipin (gift from AS Greenberg, Tufts University) were used for immunostaining. Representative micrographs were photographed at 40x magnification. Adipocyte number for each genotype was quantified by counting the total number of individual adipocytes in ten fields per mouse at 10x magnification. Liver tissues were embedded in OCT compound (Sakura Finetech USA Inc.) and frozen in liquid nitrogen. Sections were stained using standard methods for oil red O to determine lipid deposition.

Hypoxia assessment—An i.p injection of 40mg/kg pimonidazole was administered 1 hr prior to sacrifice. A portion of the EFP was fixed in 10% neutral buffered formalin, embedded in paraffin, sectioned, and stained using the Hypoxyprobe-1 Plus kit (Chemicon International) according to the manufacturer's protocol.

Quantitative PCR—A portion of the EFP was snap frozen in liquid nitrogen immediately after harvest. Tissue was disrupted using a Qiagen TissueLyser, followed by total RNA extraction using the Qiagen RNeasy Kit (Valencia, CA). cDNA was produced using ThermoScript RT-PCR Systems (Invitrogen, Carlsbad, CA). A Hypoxia PCR array (SA Biosciences) was performed according to the manufacturer's instructions and included the reported genes: Adm, Arnt2, Epo, Hif1α, Hyou1, and Notch1. Transcript levels were determined relative to the average signal from 5 supplied housekeeping genes within the test. VEGF and MMP-2 transcripts were analyzed by SYBR Green real-time PCR. The primers sequences used for qRT-PCR are: Vegf-A forward 5' ACT GGA CCC TGG CTT TAC TG 3'; Vegf-A reverse 5' TCT GCT CTC CCT CTG TCG TG 3'; MMP-2–1, 5′-GCA GGG AAT GAG TAC TGG GTC TAT-3′; and MMP-2–2 5′-CAG TTA AAG GCA GCA TCT ACT TG-3′; Sonic Hedgehog transcript was analyzed using Taqman Gene Expression Assay (#Mm00436528_m1; Applied Biosystems). Transcript levels were determined relative to the signal from GAPDH and β-actin, and normalized to the mean value of samples from wild type control mice or adiponectin-transgenic mice.

Perfusion assessment by microspheres—Anesthetized mice were injected with of 4 $\times 10^4$ yellow, 15.5μm, Dye-Trak microspheres (Triton Technology, San Diego, CA) via the left atrium. Tissues were processed according to manufacturer's protocol. Briefly, the fluorescent dye was extracted and measured with a plate reader, and normalized by the weight of each tissue depot.

Statistical Analysis—Results are shown as the mean ± SEM. Differences among groups were determined by one-way ANOVA and in cases where $P < 0.05$, an all-pairwise post hoc analysis was performed using Bonferonni's correction. Results were considered statistically

significant when $P<0.05$. Since fold-change is reported as a ratio, the statistical measures and propagation of errors was determined at a 95% confidence interval, and the upper and lower values are reported in the relevant graphs.

Results

Improved metabolic function in apn-TG mice despite diet-induced obesity— Apn-KO, wild type, and apn-TG mice were maintained on a chow diet or high fat/high sucrose (HFHS) diet for 32 weeks. Body weight did not differ among the groups when mice received chow diet (Table 1). However, as previously reported [23], EFP weight decreased in apn-TG mice (Table 1). When mice received long-term (32 weeks) HFHS diet, apn-TG mice displayed significantly increased body and EFP weight (Table 1). Circulating levels of adiponectin were found to be approximately 2-fold higher in apn-TG mice compared to wild type (Table 2), similar to those previously reported [24, 26]. In vivo metabolic parameters were assessed by insulin tolerance testing, performed on mice of all genotypes for both chow diet and HFHS diet. No differences were observed among the groups of mice receiving chow diet (data not shown). However, insulin sensitivity was affected by long-term HFHS diet. Whereas apn-KO and wild type mice maintained high levels of glucose throughout each time point, apn-TG mice demonstrated extreme insulin sensitivity, requiring removal from the experiment by the 60 minute time point (Fig. 1a). Glucose transporter type 4 (Glut4) mRNA expression was significantly higher in adipose tissue from apn-TG mice compared to apn-KO or wild type after long-term HFHS diet (Fig. 1b). Furthermore, serum insulin (Fig. 1c) and serum leptin (Fig. 1d) levels were decreased in apn-TG mice compared to apn-KO or wild type. Determination of circulating free fatty acid levels likewise revealed a significant decrease in apn-TG mice (Fig. 1e). Assessment of hepatic steatosis was determined by oil red O staining. The presence of lipid droplets in apn-KO and wild type mice was observed, while lipid droplets were virtually absent in the apn-TG mice (Fig. 1f). These data suggest that despite diet-induced obesity, a modest over-expression of adiponectin results in a healthy metabolic phenotype, both at the local and systemic level.

Decreased tissue inflammation in white adipose tissue of apn-TG mice after long-term diet-induced obesity—An indication of inflamed adipose tissue is the appearance of macrophages forming a ring around dead or dying adipocytes, described as a “crown-like structure” (CLS) [2]. Immunostaining revealed dramatically reduced macrophage content in the EFP of apn-TG mice (Fig. 2a) compared to apn-KO and wild type mice. Quantification of CLS revealed a significant reduction in adipose tissue from apn-TG (Fig. 2b). In addition, the presence of viable living cells, as determined by perilipin immunostaining, is more apparent in apn-TG mice (Fig. 2a). The extent of adipose tissue hypoxia was determined by immunohistochemical analysis using pimonidazole, which has previously been shown to quantify tissue oxygen concentration by forming adducts with thiol groups under hypoxic conditions [27]. As observed in Figure 2a, pimonidazole binding is increased in the apn-KO and wild type mice, compared to the apn-TG mice. Further characterization of adipose tissue showed an increased number of adipocytes per field in apn-TG mice compared to apn-KO and wild type mice (Fig. 2c). To further assess hypoxic conditions, whole adipose tissue mRNA levels were measured of several genes preferentially induced by hypoxia. While HIF-1α mRNA levels were marginally increased in apn-KO and wild type mice (data not shown), expression of adrenomedullin, hypoxia up-regulated 1, and matrix metalloproteinase-2 was significantly increased in apn-KO and wild type mice compared to apn-TG (Fig. 2d–f). Taken together, these data indicate that apn-TG mice maintained on long-term HFHS diet are resistant to diet-induced inflammation commonly observed in adipose tissue under obese conditions.

Elevated adiponectin increases vascularity in adipose tissue under conditions of long-term obesity—To date, no studies have examined the effects of adiponectin levels on the vascularity of the adipose tissue. Confocal visualization using isolectin Griffonia simplicifolia for the vasculature and BODIPY to identify adipocytes revealed no change in vascularization among apn-KO, wild type, and apn-TG mice maintained on chow diet (Fig. 3a). Quantification of vascularity demonstrated comparable levels among the groups (Fig. 3b). Similarly, mice maintained on short-term (10 week) HFHS diet did not differ in vascularity (data not shown). Under conditions of long-term (32 week) diet-induced obesity, confocal analysis revealed increased vascularization in apn-TG mice compared to wild type or apn-KO (Fig. 3c) and quantification demonstrated a statistically significant increase to corroborate the visual findings (Fig. 3d). To exclude the possibility that the observed angiogenic changes were due solely to conditions of obesity, vascularization was further analyzed comparing weight-matched animals from each genotype. Direct comparison showed that, as observed in Figure 3c, wild type and apn-KO mice had very low levels of vascularization within the adipose tissue, while weight-matched apn-TG mice still maintained the significantly increased vascularization observed as a group (Fig. 4).

Increased expression of angiogenic markers and perfusion in adipose tissue of adiponectin transgenic mice under conditions of long-term diet-induced obesity—The hypoxia and angiogenic related genes Arnt2, erythropoietin, and notch1 were consistently upregulated in apn-TG mice compared to apn-KO and wild type (Fig. 5a – c). Levels of vascular endothelial growth factor (VEGF), a major player in angiogenesis, were measured in EFP and also found to be increased in apn-TG mice compared to apn-KO or wild type (Fig. 5d). In addition, EFP levels of sonic hedgehog (Shh), which is known to exert postnatal angiogenic effects through upregulation of VEGF [28, 29], was also increased dramatically (Fig. 5e). Tissue perfusion was assessed by colored microsphere analysis. Relative perfusion in kidney (Fig. 5f) and heart (Fig. 5g) remained unchanged among the diet-induced obesity models, whereas the number of microspheres in the EFP of wild type and apn-KO were significantly decreased compared to apn-TG mice (Fig. 5h). Taken together, it is shown here that, under conditions of long-term diet-induced obesity, increased vascularity, angiogenic marker expression, and perfusion occurs in mice over-expressing adiponectin whereas the quantity of blood vessels in adiponectin-deficient and wild type mice is diminished.

Discussion

In this report, a modest increase in adiponectin levels enhances angiogenic potential and perfusion of white adipose tissue, which is associated with beneficial effects on metabolism when mice are subjected to diet-induced obesity. This is the first report to examine the effects of varying levels of adiponectin on adipose tissue vascularity and perfusion. While no changes were observed when mice were maintained on chow diet or short-term HFHS diet, over-expression of adiponectin resulted in increased angiogenesis and blood flow in the adipose tissue and improved systemic metabolism under conditions of long-term diet induced obesity. In addition, macrophage infiltration and evidence of hypoxia within the adipose tissue was decreased with adiponectin over-expression. These results demonstrate that increased adiponectin levels allow adipose tissue to combat adverse inflammatory conditions that normally arise with obesity, as well as preserve functional blood vessels which are known to undergo rarefaction with obesity.

It has been previously reported that adiponectin-deficiency results in insulin resistance [30] as well as exacerbation of liver disease, manifesting from metabolic syndrome, under conditions of HFHS diet [31]. Therefore, a limitation to the current study is that adiponectin deficiency did not result in worsened effects compared to wild type. It is possible that due to

the duration of the long-term HFHS diet, a severe disease state maximum occurred in both the adiponectin-deficient and wild type mice, and thus differences in phenotype became indistinguishable. However, similar to the data presented here, another group has shown that no change in insulin sensitivity occurs in adiponectin-deficient mice compared to wild type when maintained on chow diet [25]. A separate study comparing adiponectin-deficient and wild type mice maintained on HFHS diet for seven months also showed no difference in glucose tolerance or insulin resistance [32]. Therefore, although surprising, discrepancies among reports using adiponectin-deficient mice may be attributed to subtle strain differences of mice generated by independent groups.

Since a restriction of blood flow in the adipose tissue contributes to an inflammatory state, it has been proposed that adipocytes of a certain size will spontaneously undergo necrosis perhaps due to limitations in the diffusion of oxygen [2, 4]. Thus, as observed here, a reduction of adipose tissue blood flow in apn-KO and wild type mice (Fig. 4c), could promote inflammation by contributing to the necrosis of large adipocytes. Under the conditions of this study, blood flow in heart was not affected by adiponectin levels however, obesity does not affect myocardial blood flow in humans at baseline [33, 34]. Evidence also suggests a role for hypoxia in altering adipokine secretion, thereby contributing to the adipokine imbalance that is associated with obesity [3]. In the study presented here, adipose tissue of apn-TG mice contained mostly living adipocytes with virtually no CLS or evidence of hypoxia. In contrast, adipose tissue of wild type and apn-KO mice demonstrated large depots of CLS and marked hypoxia as demonstrated by binding of pimonidazole protein adducts and upregulation of genes induced by hypoxia (Fig. 2). Taken together, modest adiponectin over-expression significantly affects the dynamics of adipocyte expansion, vascularization, perfusion, and local inflammation within the adipose tissue and this could contribute to the observed beneficial changes to obesity-related metabolic dysfunction.

The study presented here examines the direct effect of adiponectin over-expression on angiogenesis in adipose tissue and demonstrates that vascularization and perfusion are increased when adiponectin levels are modestly increased. These novel findings build upon a recent study highlighting the potential importance of adiponectin-mediated angiogenesis in adipose tissue [35]. Gealekman et al., has shown that rosiglitazone, which is known to upregulate adiponectin [16], promotes ex vivo capillary growth from subcutaneous adipose tissue explants, and this was correlated with increased serum adiponectin levels. Further research is required to develop a mechanistic understanding of adiponectin-mediated angiogenesis in adipose tissue although induction of VEGF by adiponectin could potentially be mediated by Shh signaling.

In this study, I present data demonstrating that an interaction occurs between increased adiponectin expression and obesity, creating an environment which promotes angiogenesis, and the morphogen Shh could be an important factor in this process. With regard to adipocyte biology and obesity, Shh signaling elicits anti-adipogenic actions, and expression levels of Shh signaling molecules are decreased in genetic and diet-induced mouse models of obesity [36]. In addition, Shh is known to reduce lipid accumulation in adipocytes, decrease adipocyte specific gene expression, and lead to an insulin resistant state [37]. Furthermore, it has been shown that blood pressure, insulin sensitivity, and adipocyte function are improved by increased expression of adiponectin and Shh in mice maintained on a HFHS diet [38]. Cardiovascular effects of Shh include the induction of VEGF-mediated angiogenesis in the adult, under conditions of skeletal muscle ischemia and muscle regeneration [28, 29, 39]. It has also been shown that Shh treatment restores motor and sensory nerve deficits incurred by diabetic neuropathy [40]. Taken together, there is substantial evidence for Shh as a player in obesity and obesity-related complications such as vascular dysfunction, as observed in this report.

In summary, these data show that under long-term conditions of diet-induced obesity, there is a striking increase in adipose tissue vascularity and perfusion as well as diminished systemic metabolic dysfunction in mice that are genetically engineered to over-express adiponectin. Interestingly, the effect of adiponectin ablation on vascularity is negligible under conditions of long-term diet induced obesity. These data provide a foundation to begin elucidating the angiogenic signaling pathway involved in the adipocytokine control of the adipose tissue microenvironment and obesity-related inflammation.

Acknowledgments

Many thanks to Dr. Susan Fried for helpful discussion; Jennifer Parker and Zachary Weitzner for technical assistance; and Dr. Ramon Bonegio for assistance with statistics.

Funding. The project described was supported by K01 AR055965-02 grant from NIAMS/NIH to T.A.; Pilot and Feasibility Grant P30 DK046200 from the Boston Nutrition Obesity Research Center to T.A.; and National Institutes of Health UL1RR025771 from the Clinical and Translational Science Institute at Boston University to T.A. Its contents are solely the responsibility of the author and do not necessarily represent the official views of the NIAMS or NIH.

List of Abbreviations

Apn-KO	adiponectin knockout mouse
Apn-TG	adiponectin transgenic/overexpressing mouse
CLS	crown-like structure
HFHS-high	fat/high sucrose diet
IL-6	interleukin 6
Shh	Sonic Hedgehog
TNFα	tumor necrosis factor alpha
VEGF-A	vascular endothelial growth factor-A

References

1. Sun K, Kusminski CM, Scherer PE. Adipose tissue remodeling and obesity. J Clin Invest. 2011; 121(6):2094–2101. [PubMed: 21633177]
2. Cinti S, et al. Adipocyte death defines macrophage localization and function in adipose tissue of obese mice and humans. J Lipid Res. 2005; 46(11):2347–2355. [PubMed: 16150820]
3. Hosogai N, et al. Adipose tissue hypoxia in obesity and its impact on adipocytokine dysregulation. Diabetes. 2007; 56(4):901–911. [PubMed: 17395738]
4. Pasarica M, et al. Reduced adipose tissue oxygenation in human obesity: evidence for rarefaction, chemotaxis macrophage, and inflammation without an angiogenic response. Diabetes. 2009; 58(3): 718–725. [PubMed: 19074987]
5. Heilbronn LK, Campbell LV. Adipose tissue macrophages, low grade inflammation and insulin resistance in human obesity. Curr Pharm Des. 2008; 14(12):1225–1230. [PubMed: 18473870]
6. Uysal KT, et al. Protection from obesity-induced insulin resistance in mice lacking TNF-alpha function. Nature. 1997; 389(6651):610–614. [PubMed: 9335502]
7. Uysal KT, Wiesbrock SM, Hotamisligil GS. Functional analysis of tumor necrosis factor (TNF) receptors in TNF-alpha-mediated insulin resistance in genetic obesity. Endocrinology. 1998; 139(12):4832–4838. [PubMed: 9832419]
8. Gomez-Hernandez A, et al. Brown fat lipoatrophy and increased visceral adiposity through a concerted adipocytokines overexpression induces vascular insulin resistance and dysfunction. Endocrinology. 2012; 153(3):1242–1255. [PubMed: 22253415]

9. Apovian CM, et al. Adipose macrophage infiltration is associated with insulin resistance and vascular endothelial dysfunction in obese subjects. Arterioscler Thromb Vasc Biol. 2008; 28(9): 1654–1659. [PubMed: 18566296]
10. Digirolamo M, Esposito J. Adipose tissue blood flow and cellularity in the growing rabbit. Am J Physiol. 1975; 229(1):107–112. [PubMed: 1147035]
11. Ye J, et al. Hypoxia is a potential risk factor for chronic inflammation and adiponectin reduction in adipose tissue of ob/ob and dietary obese mice. Am J Physiol Endocrinol Metab. 2007; 293(4):E1118–E1128. [PubMed: 17666485]
12. Lijnen HR, et al. Impaired adipose tissue development in mice with inactivation of placental growth factor function. Diabetes. 2006; 55(10):2698–2704. [PubMed: 17003333]
13. Ouchi N, et al. Obesity, adiponectin and vascular inflammatory disease. Curr Opin Lipidol. 2003; 14:561–566. [PubMed: 14624132]
14. Berg AH, Scherer PE. Adipose tissue inflammation and cardiovascular disease. Circ Res. 2005; 96(9):939–949. [PubMed: 15890981]
15. Fasshauer M, et al. Adiponectin gene expression and secretion is inhibited by interleukin-6 in 3T3-L1 adipocytes. Biochem Biophys Res Commun. 2003; 301(4):1045–1050. [PubMed: 12589818]
16. Maeda N, et al. PPARgamma ligands increase expression and plasma concentrations of adiponectin, an adipose-derived protein. Diabetes. 2001; 50(9):2094–2099. [PubMed: 11522676]
17. Denzel MS, et al. Adiponectin deficiency limits tumor vascularization in the MMTV-PyV-mT mouse model of mammary cancer. Clin Cancer Res. 2009; 15(10):3256–3264. [PubMed: 19447866]
18. Shibata R, et al. Adiponectin stimulates angiogenesis in response to tissue ischemia through stimulation of amp-activated protein kinase signaling. J Biol Chem. 2004; 279(27):28670–28674. [PubMed: 15123726]
19. Takemura Y, et al. Adiponectin modulates inflammatory reactions via calreticulin receptor-dependent clearance of early apoptotic bodies. J Clin Invest. 2007; 117(2):375–386. [PubMed: 17256056]
20. Okamoto Y, et al. Adiponectin inhibits allograft rejection in murine cardiac transplantation. Transplantation. 2009; 88(7):879–883. [PubMed: 19935458]
21. Wilk S, et al. Adiponectin is a negative regulator of antigen-activated T cells. Eur J Immunol. 2011; 41(8):2323–2332. [PubMed: 21538348]
22. Tsang JY, et al. Novel immunomodulatory effects of adiponectin on dendritic cell functions. Int Immunopharmacol. 2011; 11(5):604–609. [PubMed: 21094289]
23. Asterholm IW, Scherer PE. Enhanced metabolic flexibility associated with elevated adiponectin levels. Am J Pathol. 2010; 176(3):1364–1376. [PubMed: 20093494]
24. Kim JY, et al. Obesity-associated improvements in metabolic profile through expansion of adipose tissue. J Clin Invest. 2007; 117(9):2621–2637. [PubMed: 17717599]
25. Maeda N, et al. Diet-induced insulin resistance in mice lacking adiponectin/ACRP30. Nat. Med. 2002; 8:731–737. [PubMed: 12068289]
26. Combs TP, et al. A transgenic mouse with a deletion in the collagenous domain of adiponectin displays elevated circulating adiponectin and improved insulin sensitivity. Endocrinology. 2004; 145(1):367–383. [PubMed: 14576179]
27. Varia MA, et al. Pimonidazole: a novel hypoxia marker for complementary study of tumor hypoxia and cell proliferation in cervical carcinoma. Gynecol Oncol. 1998; 71(2):270–277. [PubMed: 9826471]
28. Pola R, et al. The morphogen Sonic hedgehog is an indirect angiogenic agent upregulating two families of angiogenic growth factors. Nat Med. 2001; 7(6):706–711. [PubMed: 11385508]
29. Pola R, et al. Postnatal recapitulation of embryonic hedgehog pathway in response to skeletal muscle ischemia. Circulation. 2003; 108(4):479–485. [PubMed: 12860919]
30. Kubota N, et al. Disruption of adiponectin causes insulin resistance and neointimal formation. J Biol Chem. 2002; 277(29):25863–25866. [PubMed: 12032136]
31. Asano T, et al. Adiponectin knockout mice on high fat diet develop fibrosing steatohepatitis. J Gastroenterol Hepatol. 2009; 24(10):1669–76. [PubMed: 19788607]

32. Ma K, et al. Increased beta -oxidation but no insulin resistance or glucose intolerance in mice lacking adiponectin. J Biol Chem. 2002; 277(38):34658–34661. [PubMed: 12151381]

33. Schindler TH, et al. Relationship between increasing body weight, resistance, insulin inflammation, adipocytokine leptin, and coronary circulatory function. J Am Coll Cardiol. 2006; 47(6):1188–1195. [PubMed: 16545651]

34. Knudson JD, et al. Mechanisms of coronary dysfunction in obesity and insulin resistance. Microcirculation. 2007; 14(4–5):317–338. [PubMed: 17613805]

35. Gealekman O, et al. Effect of rosiglitazone on capillary density and angiogenesis in adipose tissue of normoglycaemic humans in a randomised controlled trial. Diabetologia. 2012; 55(10):2794–2799. [PubMed: 22847059]

36. Suh JM, et al. Hedgehog signaling plays a conserved role in inhibiting fat formation. Cell Metab. 2006; 3(1):25–34. [PubMed: 16399502]

37. Fontaine C, et al. Hedgehog signaling alters adipocyte maturation of human mesenchymal stem cells. Stem Cells. 2008; 26(4):1037–1046. [PubMed: 18258719]

38. Cao J, et al. Heme oxygenase gene targeting to adipocytes attenuates adiposity and vascular dysfunction in mice fed a high-fat diet. Hypertension. 2012; 60(2):467–475. [PubMed: 22753217]

39. Straface G, et al. Sonic hedgehog regulates angiogenesis and myogenesis during postnatal skeletal muscle regeneration. J Cell Mol Med. 2009; 13(8B):2424–2435. [PubMed: 18662193]

40. Kusano KF, et al. Sonic hedgehog induces arteriogenesis in diabetic vasa nervorum and restores function in diabetic neuropathy. Arterioscler Thromb Vasc Biol. 2004; 24(11):2102–2107. [PubMed: 15358602]

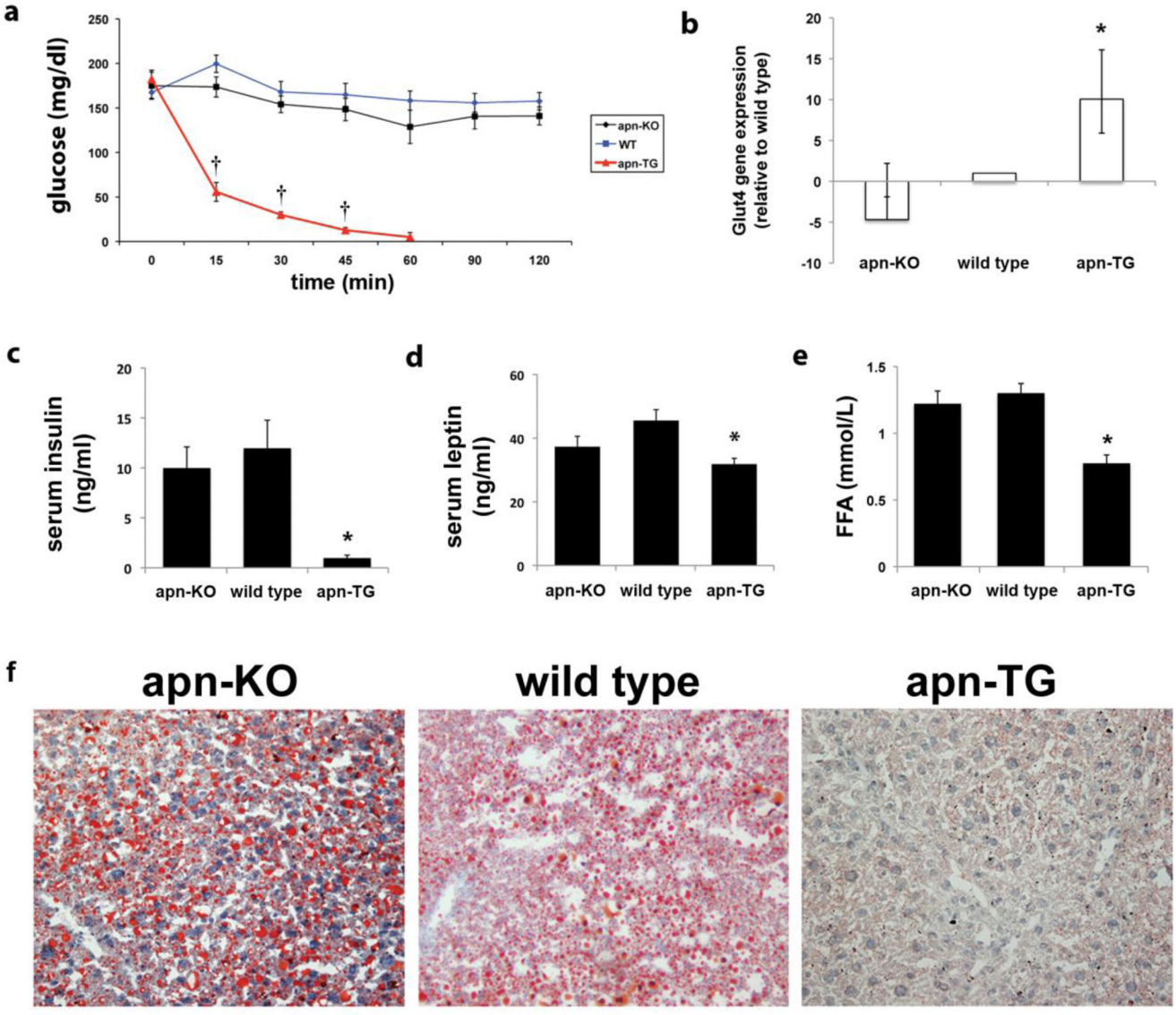

Figure 1.

Increased adiponectin improves systemic metabolism under conditions of long-term diet-induced obesity. a) Insulin tolerance test was performed on mice after overnight fasting. b) mRNA expression levels of Glut4 were determined in epididymal fat pads from mice in each group and are expressed as relative to wild type with upper and lower confidence intervals represented. c) Endpoint serum levels of insulin, d) leptin, and e) free fatty acids were assessed using commercially available assays. f) Sections from apn-deficient (apn-KO), wild type, and adiponectin over-expressing (apn-TG) liver were stained with oil red O. Data are shown as means ± SEM and represent apn-KO (n=9); wild type (n=11); apn-TG (n=8) *P<0.05, vs. apn-KO and wild type; †P<0.001, vs. apn-KO and wild type.

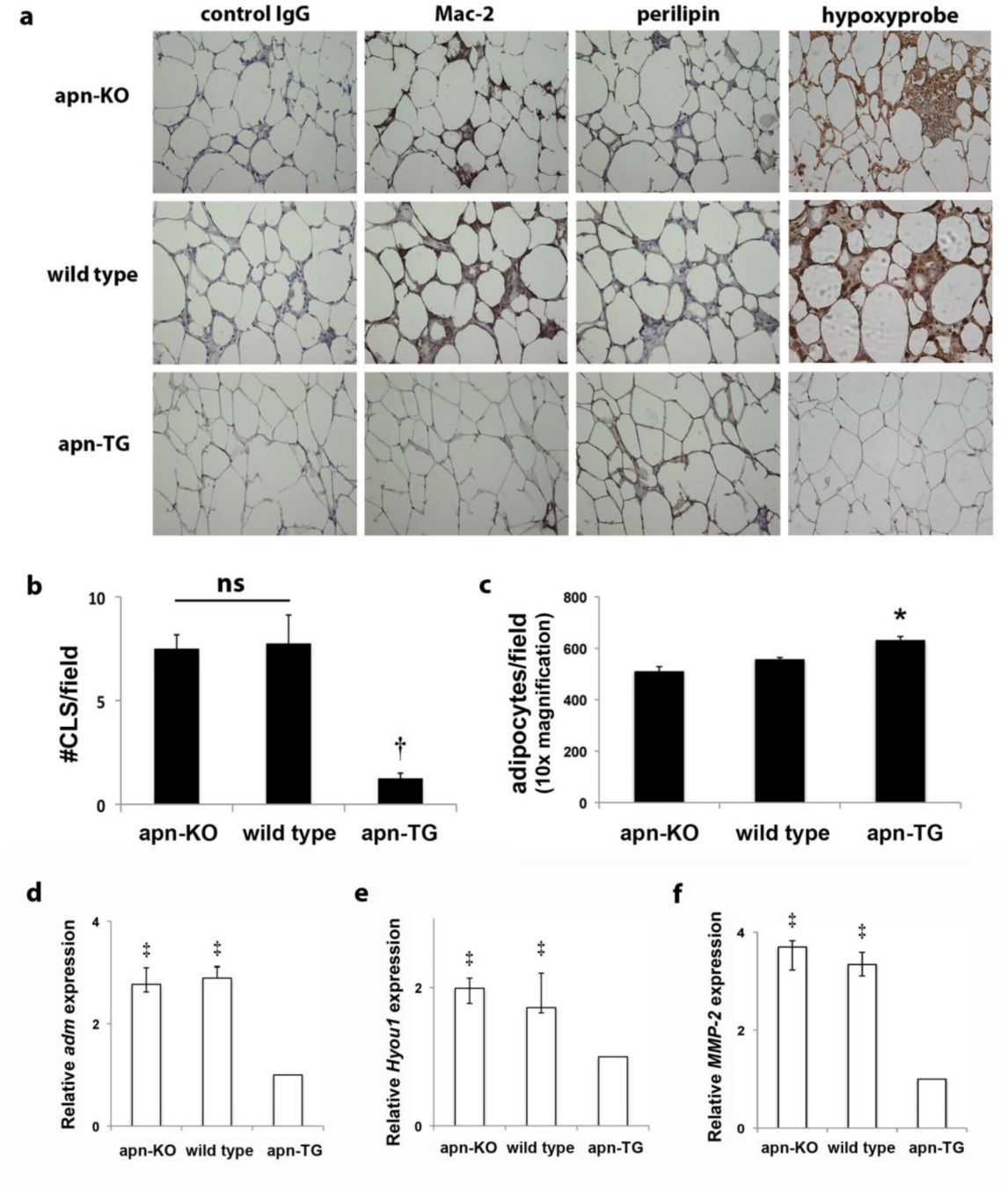

Figure 2.

Mice over-expressing adiponectin are protected from adipose tissue inflammation after long-term high fat/high sucrose diet. a) Representative micrographs (40x magnification) from serial sections of adiponectin-deficient (apn-KO) (n=9), wild type (n=11), and adiponectin-overexpressing (apn-TG) (n=8) mice stained with control IgG, Mac-2 for macrophages or perilipin for viable adipocytes. Dead or dying adipocytes are identified as perilipin-negative lipid droplets surrounded by macrophage crowns. Additional slides show pimonidazole protein adducts, visualized by brown staining. b) The number of crown-like structures was quantified per field for each group. c) Total adipocyte count per field (10x magnification). Whole adipose tissue gene expression of d) adrenomedullin (adm), e) hypoxia up-regulated

1 (Hyou1), and f) matrix metalloproteinase-2 (MMP-2) was quantified by RT-PCR. Data are shown as means ± SEM and represent apn-KO (n=9); wild type (n=11); apn-TG (n=8) *$P<$ 0.05 vs. apn-KO and wild type; †$P<0.001$ vs. apn-KO and wild type; ‡$P<0.001$ vs. apn-TG.

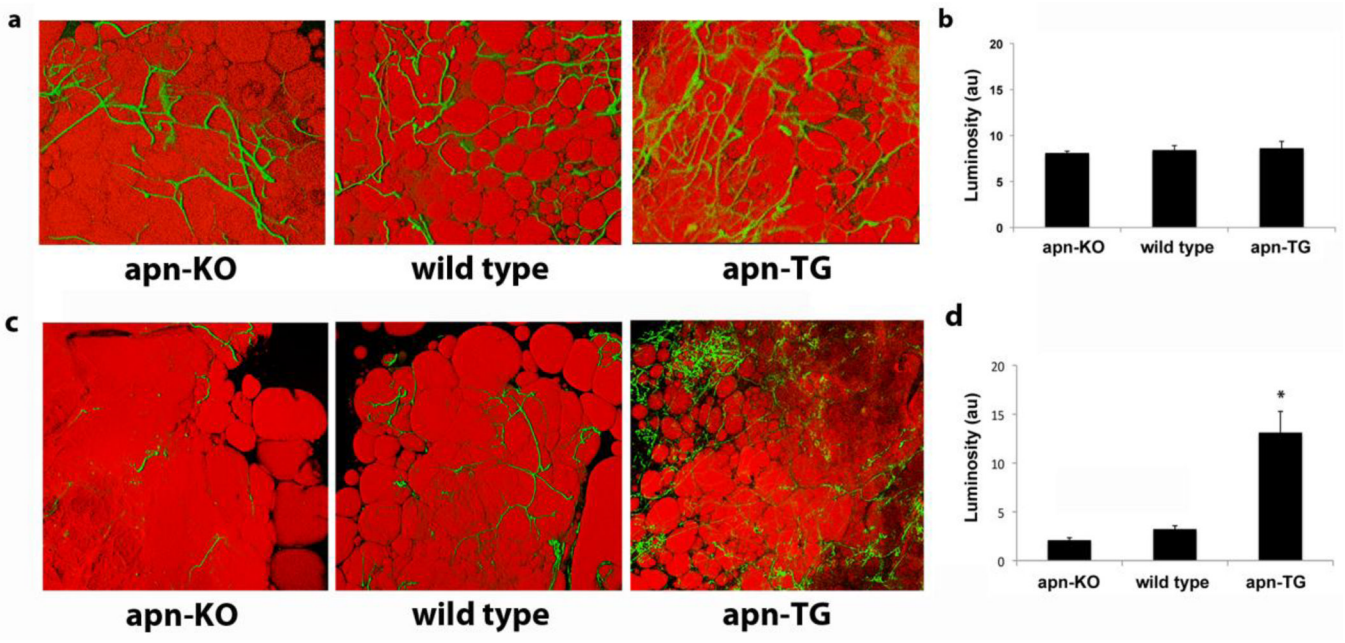

Figure 3.

Adipose tissue angiogenesis in mice with varying adiponectin levels under conditions of chow diet or high fat/high sucrose diet. a) Representative confocal micrographs of epididymal fat pads excised from adiponectin-deficient (apn-KO) (n=6), wild type (n=11), and adiponectin-over-expressing (apn-TG) (n=5) mice, maintained on chow diet. Tissue was stained with BS1-lectin–FITC (green) for vasculature, and BODIPY-TR (red) for adipocytes. b) Quantification of FITC luminosity indicating capillary density. c) Representative confocal micrographs of adipose tissue stained with BS1-lectin (green) for vasculature, and BODIPY-TR (red) for adipocytes from adiponectin-deficient (apn-KO) (n=9), wild type (n=11), and adiponectin-over-expressing (apn-TG) (n=8) mice after 32 weeks high fat/high sucrose diet. d) Quantification of FITC luminosity indicating capillary density. Data are shown as means ± SEM. *P<0.001 vs. apn-KO and wild type.

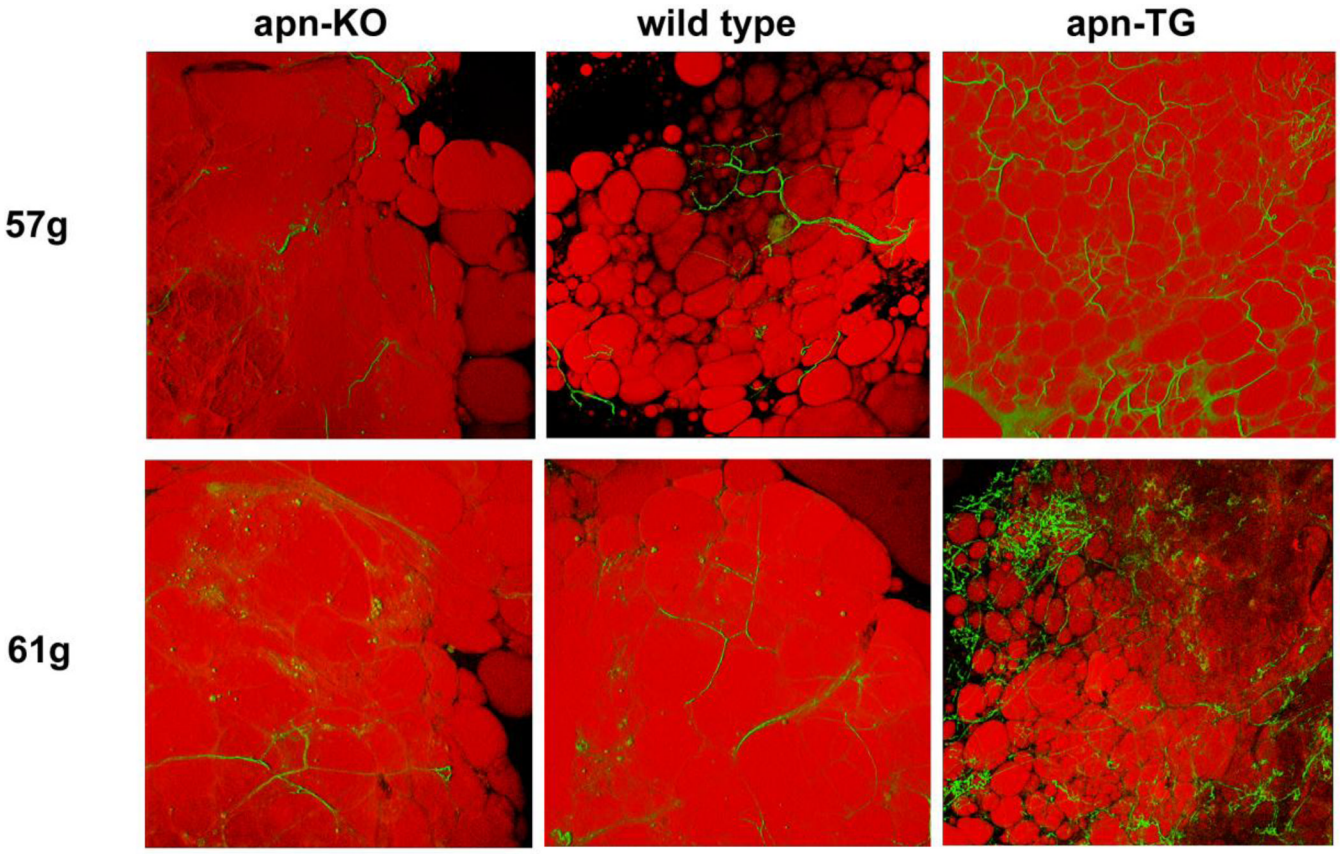

Figure 4.
Relationship between obesity and vascularity in adipose tissue. Vascularity was compared in confocal images from weight-matched animals of each genotype maintained on long-term HFHS diet.

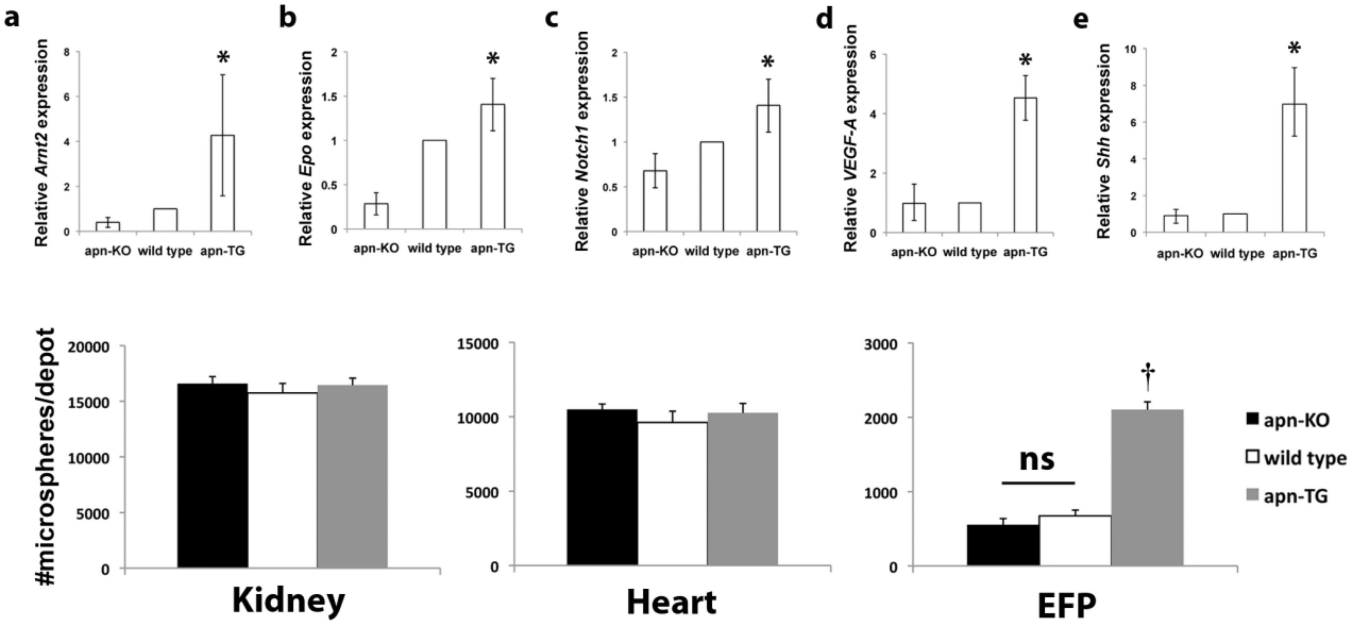

Figure 5.

Adiponectin levels affect angiogenic marker expression and perfusion in adipose tissue after long-term maintenance on high fat/high sucrose diet. a–c) Selected relevant mRNA levels in epididymal fat pad (EFP) of genes involved in hypoxic and angiogenic pathways as determined by PCR array, expressed relative to wild type and shown with upper and lower confidence intervals. d) Whole adipose tissue gene expression of d) VEGF and e) Shh was quantified by RT-PCR. Tissue perfusion was determined by quantifying number of microspheres in f) kidney, g) heart, and h) EFP. Data are shown as means ± SEM and represent apn-KO (n=9), wild type (n=11), and apn-TG (n=8) *P<0.01 vs. apn-KO and wild type; †P<0.001 vs. apn-KO and wild type.

Table 1

Body and adipose tissue weight (g)

	apn-KO		Wild type		apn-TG	
	Chow Diet	**HFHS Diet**	**Chow Diet**	**HFHS Diet**	**Chow Diet**	**HFHS Diet**
Body	42.7±2.12	55.5±1.09	46.4±1.35	55.6±1.43	43.7±3.42	67.0±3.24 *
EFP	1.82±0.28	1.49±0.7	2.26±0.10	1.27±0.06	0.60±0.11 †	2.25±0.30 ‡

Values reported are mean ± SEM. *P* values reflect comparisons between indicated groups by ANOVA.

* *P*<0.001 versus apn-KO and wild type on HFHS diet

† *P*<0.001 versus apn-KO and wild type on chow diet

‡ *P*<0.001 versus apn-KO and wild type on HFHS diet

Metabolism. Author manuscript; available in PMC 2014 December 01.

Table 2

Adiponectin expression (μg/ml)

	apn-KO		Wild type		apn-TG	
	Chow Diet	**HFHS Diet**	**Chow Diet**	**HFHS Diet**	**Chow Diet**	**HFHS Diet**
Serum	Nd	nd	11.2±2.79	6.37±3.82 *	26.4±5.47 *	29.6±6.21 †

Values reported are mean ± SEM. *P* values reflect comparisons between indicated groups by ANOVA.

* *P*<0.01 versus wild type on chow diet

† *P*<0.001 versus wild type on HFHS diet

nd = non-detectable